0273-2289/91/2829—0699$04.00

A Structured Model for Vegetative Growth and Sporulation in *Bacillus thuringiensis*

MACIEJ STARZAK AND RAKESH K. BAJPAI*

Department of Chemical Engineering, University of Missouri-Columbia, 1030 Engineering Bldg., Columbia, MO 65211

ABSTRACT

A mathematical model has been developed for the δ-endotoxin producing *Bacillus thuringiensis*. The structure of the model involves the processes taking place during vegetative growth, those leading to the initiation of sporulation under conditions of carbon and/or nitrogen limitation, and the sporulation events. The key features in the model are the pools of compounds, such as PRPP, IMP, ADP/ATP, GDP/GTP, pyrimidine nucleotides, NAD/$NADH_2$, amino acids, nucleic acids, cell wall, and vegetative and sporulation proteins. These, along with σ-factors that control the nature of RNA-polymerase during the different phases, effectively stimulate the vegetative growth and sporulation. The initiation of sporulation is controlled by the intracellular concentration of GTP. Results of simulation of vegetative growth, initiation of sporulation, spore protein formation, and production of δ-endotoxin under C- or N-limitation are presented.

Index Entries: *Bacillus thuringiensis;* vegetative growth; sporulation; δ-endotoxin; structured model.

NOMENCLATURE

a_i	mass fraction of *i*-th intracellular component, g/g D.W.
c_i	concentration of *i*-th extracellular component in broth, g/dm^3
i	inhibition constant
k	maximum reaction rate constant, h^{-1}
K	saturation constant (for intracellular conditions of vegetative growth)
K^*	saturation constant (for intracellular conditions of sporulation)

*Author to whom all correspondence and reprint requests should be addressed.

K	equilibrium constant
m_e	maintenance coefficient, mol ATP/g D.W./h
r_i	rate of i-th reaction, g/g D.W./h
R_i	net formation rate of *i*-th component, g/g D.W./h
t	time, h
X	biomass concentration, g/dm^3
Y_{ji}	stoichiometric mass yield coefficient for *i*-th component in *j*-th reaction
μ	specific growth rate, h^{-1}
Ace	acetate
AmA	amino acids
CE	core enzyme
G	glucose
I	GTP-binding protein
Lac	lactate
N	ammonia
NA	nucleic acids
P_c	crystal protein (δ-endotoxin)
P_i	inorganic phosphate (H_3PO_4)
P_s	spore protein
P_v	vegetative protein
PTP	pyrimidine nucleotides
π	RNA-polymerase
σ	sigma factor

INTRODUCTION

A series of biochemically structured "single-cell" models for different microorganisms has been proposed recently (*1–3*). All these models can describe the metabolism of a single cell and behavior of biomass as a whole during vegetative growth, including both the exponential and stationary phase, as well as transient states. The present study is an attempt to apply this approach to simulate sporulating bacteria.

An interesting and industrially important representative of sporulating microorganisms is *Bacillus thuringiensis* (*Bt.*) var. *kurstaki*. It produces an intracellular parasporal crystal protein, known as δ-endotoxin, and is widely used as a bioinsecticide (*4–6*). Although, δ-endotoxin has been commercially produced for many years, the present technology for its production still involves batch processing. Alternative schemes, such as fed-batch operation, can improve the efficiency significantly and need to be explored. The mathematical model to be developed here should permit exploration, optimization, and control of new prospective fermentation technologies for the δ-endotoxin production.

CHARACTERISTICS OF THE BACTERIUM

Bacillus thuringiensis var. *kurstaki* is a gram-positive, spore-forming aerobic bacterium that can grow on synthetic media (glucose-salts) sup-

plemented with glutamate or natural amino acid rich components. To catabolize glucose, the bacterium uses mainly the EMP pathway (*7*). Glucose is consumed in catabolic processes to produce acetic acid, lactic acid, and carbon dioxide, as well as small amounts of pyruvic acid and acetoin (*8*). *Bt.* has an incomplete TCA cycle owing to the absence of the α-ketoglutarate dehydrogenase (*9*). Glyoxylate cycle is very active, as indicated by high activities of isocitrate lyase and malate synthase. Glyoxylate produced in this situation is most probably metabolized by conversion to tartronic semialdehyde and then to glyceric acid (*10*). In genus *Bacillus*, the conversion of acetyl-CoA to acetate is catalyzed by phosphotransacetylase and acetate kinase with the formation of only one molecule of ATP (*11*). Cytochrome system in *Bt.* probably involves three energy coupling sites for ATP resynthesis (mechanistic ratio P/O=3) (*12*).

Besides the classic cell division during vegetative growth, the life cycle of this microorganism can also include the process of spore formation (*4–6,13*). Massive sporulation may be initiated by deprivation of key nutrients, such as glucose, ammonia, or phosphate. Weak sporulation occurs to some extent during vegetative growth also (*14,15*). This type of sporulation does not seem to require any specific initiation. Sporulation is accompanied by synthesis of δ-endotoxin. This crystal protein is produced mainly during stages III (forespore engulfment) and IV (cortex formation) of the process, and is a sporulation-specific event.

MATHEMATICAL MODELS OF SPORULATING BACTERIA

Only a few mathematical models have been proposed for sporulating bacteria (*16–18*). In all cases, the proposed models were unstructured and intracellular metabolism was not considered. The process of sporulation was initiated by the exhaustion of limiting nutrient. In fact, the models were segregated. They included three or four populations: vegetative cells, cells initiated to form spores, cells containing observable spores + free spores, and eventually cells with visible protein crystals. The appearance of subsequent populations following vegetative growth was timed by appropriately selected time delays. Vegetative growth was described by substrate-limited Monod kinetics, whereas first-order kinetics was assumed for sporulation processes. Regulation of synthesis of different proteins was not considered. Therefore, these mathematical models are restricted in their applications. We hope that structured models will allow for more reliable extrapolation and be capable of simulating a wider range of conditions.

Very recently, Jeong et al. (*3*) have described a highly structured model for growth process of *B. subtilis*. The model is capable of simulating vegetative growth of the bacterium, including the transition between exponential and stationary phases of growth in a batch culture. It is based on very detailed studies of cell metabolism. Since GTP has been recognized as

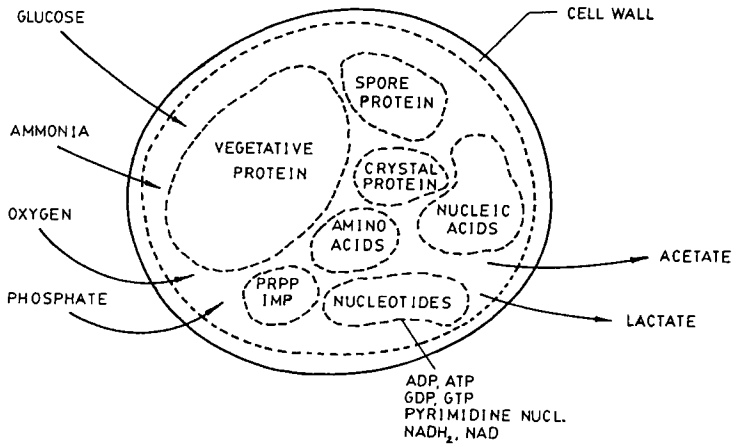

Fig. 1. Intracellular pools.

one of the most probable effector molecules that may provide the signal for the initiation of sporulation, purine metabolism was considered in detail. Yet, the model does not involve sporulation phenomena. Simulations revealed irregular aperiodic oscillatory behavior for most of intracellular concentrations, which might have resulted from the uncertainty of an enormous set of kinetic data used. The concentration of GTP, a potential repressor of the initiation process, increased at the end of exponential growth instead of decreasing as had been observed experimentally (*19,20*). Nevertheless, the study is an excellent starting point for seeking more realistic and, if possible, less complex mathematical models of sporulating bacteria.

STRUCTURED MODEL DEVELOPMENT

General Assumptions

The model of *Bt.* described here is biochemically structured and nonsegregated. Consequently, no distinction is made between nonsporulating and sporulating cells. During sporulation, the content of newly synthesized proteins within the cell increases and that of old vegetative protein drops. Each cell, however, is equally advanced in its spore formation process. This limitation of the model does not allow for separate prediction of vegetative cells and spore counts.

The model considers several intracellular pools. These and the compounds recognized as extracellular (nutrients and final metabolic products) have been shown in Fig. 1. The pool of nucleic acids involves DNA as well as all the forms of ribonucleic acids. Similarly, the pools of nucleotides include deoxyribonucleotides also. The model ignores intracellular morphology and considers the cell a single compartment in which all the defined pools are perfectly mixed.

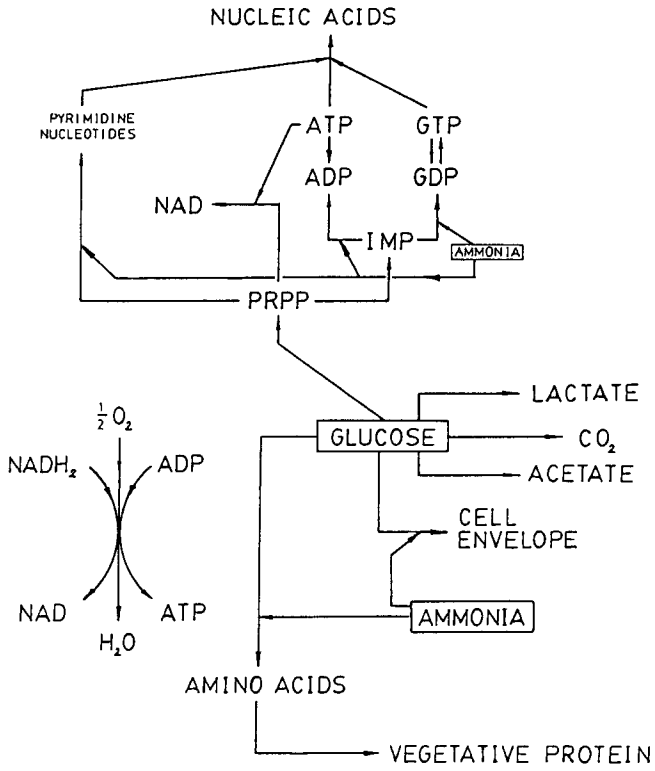

Fig. 2. Metabolic flow-chart (vegetative growth).

We endeavored also to make the model consistent with what is currently known about cell energetics. As a result, the rates of all anabolic processes occurring in the cell are influenced by energy carriers (ATP or GTP), which in turn, via the respiratory system, are coupled with the reaction flow of reducing equivalents ($NADH_2$).

Vegetative Growth

A metabolic flow-chart is shown in Fig. 2. It is assumed that glucose and ammonia are limiting nutrients. Other nutrients necessary for normal growth (oxygen, phosphate, specific amino acids, and mineral components) are present in excess.

Nucleotide synthesis makes up an important part of the metabolic scheme. It has been split into ATP, GTP, and pyrimidine nucleotide synthesis with PRPP as a common precursor. It is worth noting (Fig. 2) that GTP synthesis depends on the presence of both the key nutrients (glucose and ammonia) in the fermentation medium. This limitation is crucial while discussing the trigger mechanism of sporulation. Synthesis of dinucleotides is also considered; however, no distinction has been made between different reducing power carriers ($NADH_2$, $NADPH_2$, $FADH_2$).

Ammonia uptake is considered to involve energetic costs. Transport of glucose requires no additional energy expenditure, since glucose is

converted into glucose-6-phosphate during its uptake from broth. Maintenance energy requirements have been accounted for by natural hydrolysis of ATP and GTP.

The stoichiometry of vegetative growth reactions is presented in Table 1. Stoichiometric coefficients for synthesis of amino acids, cell wall, pyrimidine nucleotides, nucleic acids, and proteins have been obtained from available cell composition data (*24*).

The reaction rate equations are shown in Table 2. Most of the reactions have been assumed to be irreversible. Nucleic acids undergo degradation mainly owing to high m-RNA instability (*25*). A slow decay of vegetative protein has also been considered (*26*). Generally, the Michaelis-Menten (multiple-saturation type) kinetics has been used to express reaction rates. First-order kinetics was assumed for hydrolysis and degradation processes. Since only a few of the saturation constants could be determined directly from the literature, all of them were estimated by assuming 1/25 of the normal intracellular concentration of corresponding species during exponential growth (*27*). A small number of inhibition constants has been taken from ref. (*3*). A more detailed discussion of vegetative growth will be presented elsewhere (*24*).

Regulation of Protein Synthesis

It is assumed that three basic kinds of proteins appear in the life cycle of *Bt.*: vegetative proteins, spore proteins, and crystal protein. Genes associated with these proteins are expressed at different times in accordance with the differentiation scenario of sporulating organism (*28*).

Initiation of transcription, which involves RNA-polymerase (π), is assumed to be a rate-controlling step for protein synthesis. A number of RNA-polymerases are present in sporulating bacteria, depending on the phase of growth. These differ mainly in the σ-factor involved, which along with core enzyme (CE) form the components of the polymerase holoenzyme ($CE + \sigma \leftrightharpoons \pi$). Up to nine different σ-factors have been reported for *B. subtilis* (*29,30*). σ^A is the predominant factor present in vegetative cells, and π^A is the polymerase likely to direct most of the RNA synthesis during vegetative growth. σ^B, σ^C, and σ^D have also been found in vegetative cells; however, holoenzymes carrying these subunits compose only a very small fraction of the extractable polymerase during vegetative phase.

A cascade of σ-factors controls sporulation events. The two basic σ-factors involved in the initiation and first period of sporulation are σ^H and σ^E. The π^H polymerase controls synthesis of genes for the stage of septation, as well as directs the synthesis of σ^E. In turn, the π^E polymerase produces genes for a later differential development of spore formation (*29*).

Sporulation-specific σ-factors (σ^H and σ^E) exhibit a much stronger affinity for the core enzyme (CE) than vegetative ones. As a result, no π^A vegetative polymerase can be found during sporulation. However, free σ^A factors can be recovered from extracts of sporulating cells (*31*).

The synthesis of crystal toxin of *Bt.* is a sporulation-specific phenomenon. Not only do the times of appearance of the spore and crystal overlap, but they are also formed in close proximity. However, it cannot be excluded that the processes of spore and crystal proteins formation are decoupled, since it was found these proteins were encoded by different genes and synthesized by different m-RNAs (*5,6*). Like most other proteins, synthesis of the crystal toxin is apparently controlled at the level of transcription.

It can be concluded from this brief discussion that the mechanism of protein synthesis in sporulating *Bt.* is very complex. For the purpose of modeling, the following simplified picture of the real mechanism can be proposed:

- π^A is the only polymerase responsible for the synthesis of vegetative protein
- Weak sporulation does not require any initiation and is catalyzed by π^B polymerase
- Carbon and/or nitrogen limitations initiate indirectly σ^E synthesis, which, in turn, causes onset of massive sporulation
- π^E polymerase catalyzes both synthesis of spore and crystal proteins
- Association between the σ-factors and the core enzyme is a fast equilibrium process with substantially different equilibrium constants for different σ-factors ($\mathbf{K_A} << \mathbf{K_B} << \mathbf{K_E}$).

It is assumed that the total intracellular concentrations (including both free and bound forms) of σ-factors σ^A and σ^B, and core enzyme remain constant. The dynamics of σ_t^E, the total concentration of σ^E, is assumed to be governed by the following differential equation:

$$\frac{d}{dt}(\sigma_t^E) = r_E - \mu \sigma_t^E, \qquad \sigma_t^E(0) = 0 \tag{1}$$

where r_E is the net rate of σ^E formation.

It is also assumed that the association equilibria ($CE + \sigma \rightleftharpoons \pi$) are attained instantaneously. Under these conditions, it can be shown that the concentration of free core enzyme (CE) depends only on σ_t^E. A detailed mathematical analysis of competitive binding of different sigmas to the common core enzyme together with the concomitant synthesis of σ^E factor will be presented elsewhere (*32*).

Trigger Mechanism for Massive Sporulation

GTP has been postulated to constitute a signal controlling initiation of sporulation (*20*). It is assumed that GTP affects the initiation through a specific activator protein *I* (*33,34*). It is uncertain whether a decrease in GTP levels causes an activation or a derepression of sporulation genes (*20,35*). In the first, the protein acts as an inducer, whereas the GTP-protein complex is an inert substance. In the second scenario, the GTP-protein

Table 1
Stoichiometry of Vegetative Growth Reactions

1. Total glucose dissimilation to carbon dioxide in the modified TCA cycle (via glyoxylate and glycerate)
   $Glucose + 2\ ADP + 2\ P_i + 12\ NAD + 4\ H_2O \longrightarrow 6\ CO_2 + 2\ ATP + 12\ NADH_2$

2. Acetate formation
   $Glucose + 4\ ADP + 4\ P_i + 4\ NAD \longrightarrow 2\ Acetate + 2\ CO_2 + 4\ ATP + 4\ NADH_2 + 2\ H_2O$

3. Lactate formation
   $Glucose + 2\ ADP + 2\ P_i \longrightarrow 2\ Lactate + 2\ ATP + 2\ H_2O$

4. Amino acid (AmA) synthesis, $M_{AmA} = 129.20$ g/mol
   $0.924\ Glucose + 1.358\ NH_3 + 0.529\ ATP + 0.779\ NAD \longrightarrow AmA + 0.529\ (ADP + P_i) + 0.779\ NADH_2$

5. Cell wall synthesis, $M_{monomer} = 1065.73$ g/mol, $M_{AmA} = 174.99$ g/mol
   (AmA = 1.070 alanine + 0.535 glutamate + 0.009 serine)
   $6.54\ Glucose + 4.52\ NH_3 + AmA + 12.82\ ATP + 4.95\ NAD \longrightarrow Cell\ wall\ monomer + 12.82\ (ADP + P_i) + 4.95\ NADH_2$

6. PRPP (phosphoribosylpyrophosphate) synthesis from glucose
   $Glucose + 3\ ATP + 2\ NAD + H_2O \longrightarrow PRPP + 3\ ADP + 2\ NADH_2 + CO_2$

7. IMP (inosine monophosphate) synthesis from PRPP, $M_{AmA} = 135.11$ g/mol (AmA = 2 serine - glycine)
   $PRPP + 3\ NH_3 + AmA + 6\ ATP + CO_2 + 2\ H_2O \longrightarrow IMP + 6\ ADP + 8\ P_i + 2\ NADH_2$

8. ADP (adenosine diphosphate) synthesis from IMP
   $IMP + NH_3 + GTP \longrightarrow ADP + GDP + H_2O$

9. ATP (adenosine triphosphate) natural hydrolysis
   $ATP + H_2O \longrightarrow ADP + P_i$

10. GDP (guanosine diphosphate) synthesis from IMP
    $IMP + NH_3 + 3\ ATP + NAD + 2\ H_2O \longrightarrow GDP + 3\ ADP + 2\ P_i + NADH_2$

11. GTP (guanosine triphosphate) synthesis from GDP
    $GDP + ATP \longrightarrow GTP + ADP$

12. GTP natural hydrolysis
$GTP + H_2O \longrightarrow GDP + P_i$

13. Synthesis of pyrimidine nucleotides (PTP), M_{PTP} = 482.85 g/mol, M_{AmA} = 133.10 g/mol (AmA = Aspartate)
$PRPP + AmA + 1.452\ NH_3 + 6.021\ ATP + 0.878\ NAD \longrightarrow PTP + 6.021\ (ADP + P_i) + 0.878\ NADH_2$

14. Synthesis of nucleic acids (NA), M_{NA} = 1288.28 g/mol
$(1.031 + 2.042)\ ATP + 1.165\ GTP + 1.797\ PTP \longrightarrow NA + 2.042\ ADP + 10.042\ P_i$

15. NAD synthesis, M_{AmA} = 115.14 g/mol (AmA = tryptophan - alanine)
$PRPP + AmA + NH_3 + 3\ O_2 + 4\ ATP + 4\ H_2O \longrightarrow NAD + 3\ ADP + 7\ P_i + 2\ CO_2$

16. Synthesis of vegetative protein, M_{AmA} = 131.21 g/mol, M_{pept} = 113.20 g/mol
$AmA + (2 + \alpha)\ ATP + 2\ GTP + (3 + \alpha)\ H_2O \longrightarrow$ Peptide monomer $+ (2 + \alpha)\ ADP + 2\ GDP + (4 + \alpha)\ P_i$
α = 0.124 accounts for proofreading, assembly and modification reactions (*21*).

17. Oxidative phosphorylation ($\delta = 3 \times 67.5\%$, see Roels (*22*))
$\frac{1}{2}\ O_2 + NADH_2 + \delta\ (ADP + P_i) \longrightarrow NAD + \delta\ ATP + (1+\delta)\ H_2O$

18. Degradation of nucleic acids
$NA + 5.790\ ATP \longrightarrow 1.165\ GDP + 1.797\ PTP + (1.031 + 5.790)\ ADP$

19. Degradation of vegetative protein, M_{AmA} = 131.21 g/mol
Peptide monomer $+ H_2O \longrightarrow AmA$

20. Transport processes (½ mole of ATP per one mole of ammonia uptaken (*23*))

Table 2
Reaction Rates of Vegetative Growth
(reference species are given in parentheses)

$$r_1 = k_1 \frac{G}{G + K_G} \frac{ADP}{ADP + K_{ADP}} \frac{NAD}{NAD + K_{NAD}} \quad \text{(glucose)}$$

$$r_2 = k_2 \frac{G}{G + K_G} \frac{ADP}{ADP + K_{ADP}} \frac{NAD}{NAD + K_{NAD}} \frac{I_{Ac}}{Ac + I_{Ac}} \quad \text{(glucose)}$$

$$r_3 = k_3 \frac{G}{G + K_G} \frac{ADP}{ADP + K_{ADP}} \frac{I_{Lac}}{Lac + I_{Lac}} \quad \text{(glucose)}$$

$$r_4 = k_4 \frac{G}{G + K_G} \frac{N}{N + K_N} \frac{ATP}{ATP + K_{ATP}} \frac{NAD}{NAD + K_{NAD}} \frac{I_{AmA}}{AmA + I_{AmA}} \frac{I_{Ac}}{Ac + I_{Ac}} \quad \text{(glucose)}$$

$$r_5 = k_5 \frac{G}{G + K_G} \frac{N}{N + K_N} \frac{AmA}{AmA + K_{AmA}} \frac{ATP}{ATP + K_{ATP}} \frac{NAD}{NAD + K_{NAD}} \quad \text{(glucose)}$$

$$r_6 = k_6 \frac{G}{G + K_G} \frac{ATP}{ATP + K_{ATP}} \frac{NAD}{NAD + K_{NAD}} \left[\frac{I_{PRPP}}{PRPP + I_{PRPP}} \right]^2 \quad \text{(glucose)}$$

$$r_7 = k_7 \frac{PRPP}{PRPP + K_{PRPP}} \frac{N}{N + K_N} \frac{AmA}{AmA + K_{AmA}} \frac{ATP}{ATP + K_{ATP}} \frac{I_{IMP}}{IMP + I_{IMP}} \quad \text{(PRPP)}$$

$$r_8 = k_8 \frac{IMP}{IMP + K_{IMP}} \frac{N}{N + K_N} \frac{GTP}{GTP + K_{GTP}} \frac{I_{ADP}}{ADP + I_{ADP}} \quad \text{(IMP)}$$

$$r_9 = k_9 \, ATP \quad \text{(ATP)}$$

$$r_{10} = k_{10} \frac{IMP}{\overline{IMP} + K_{IMP}} \frac{N}{\overline{N} + K_N} \frac{ATP}{\overline{ATP} + K_{ATP}} \frac{NAD}{\overline{NAD} + K_{NAD}} \frac{i_{GDP}}{\overline{GDP} + i_{GDP}} \quad \text{(IMP)}$$

$$r_{11} = k_{11} \frac{GDP}{\overline{GDP} + K_{GDP}} \frac{ATP}{\overline{ATP} + K_{ATP}} \frac{i_{GTP}}{\overline{GTP} + i_{GTP}} \quad \text{(GDP)}$$

$$r_{12} = k_{12} \text{ GTP} \quad \text{(GTP)}$$

$$r_{13} = k_{13} \frac{PRPP}{\overline{PRPP} + K_{PRPP}} \frac{AmA}{\overline{AmA} + K_{AmA}} \frac{N}{\overline{N} + K_N} \frac{ATP}{\overline{ATP} + K_{ATP}} \times \frac{NAD}{\overline{NAD} + K_{NAD}} \frac{i_{PTP}}{\overline{PTP} + i_{PTP}} \quad \text{(PTP)}$$

$$r_{14} = k_{14} \frac{ATP}{\overline{ATP} + K_{ATP}} \frac{GTP}{\overline{GTP} + K_{GTP}} \frac{PTP}{\overline{PTP} + K_{PTP}} \quad \text{(NA)}$$

$$r_{15} = k_{15} \frac{PRPP}{\overline{PRPP} + K_{PRPP}} \frac{AmA}{\overline{AmA} + K_{AmA}} \frac{N}{\overline{N} + K_N} \frac{ATP}{\overline{ATP} + K_{ATP}} \quad \text{(NAD)}$$

$$r_{16} = k_{16} \pi^A \frac{AmA}{\overline{AmA} + K_{AmA}} \frac{ATP}{\overline{ATP} + K_{ATP}} \frac{GTP}{\overline{GTP} + K_{GTP}} \quad \text{(AmA)}$$

$$r_{17} = k_{17} \frac{NADH_2}{\overline{NADH_2} + K_{NADH_2}} \frac{ADP}{\overline{ADP} + K_{ADP}} \frac{i_{ATP}}{\overline{ATP} + i_{ATP}} \quad \text{(ATP)}$$

$$r_{18} = k_{18} \text{ NA} \frac{ATP}{\overline{ATP} + K_{ATP}} \quad \text{(NA)}$$

$$r_{19} = k_{19} P_v \quad \text{(AmA)}$$

complex is an active repressor of sporulation genes. In any case, the mathematical form representing the effect of GTP can be approximated by

$$I = \frac{I_0}{1 + K_I (GTP)^n} \tag{2}$$

where K_I is the equilibrium constant of the complexing reaction and I_0 is the concentration of total activator protein in the cells, which has been assumed to be constant (32). During vegetative growth when normal GTP concentrations occur (0.6–1.2 m*M*), *I* is practically zero. Therefore, during this time σ^E synthesis is impossible. In turn, when GTP concentration drops because of nutrient limitation, *I* approaches I_o, resulting in formation of σ^E and initiation of sporulation. No information is available about stoichiometry of the GTP binding. We postulated that the reaction between GTP and the protein involved three GTP molecules ($n=3$).

The factor *I* controls the rate of synthesis of σ^E. The net rate of formation (r_E) of σ^E is then

$$r_E = k_E^+ I \frac{AmA}{AmA + K^*_{AmA}} - k_E^- \sigma^E \tag{3}$$

where the second term of Eq. (3) represents the rate of σ^E degradation. The idea of trigger mechanism and protein synthesis regulation has been shown schematically in Fig. 3.

Sporulation Phase Kinetics

The kinetics of different processes during sporulation has been modeled in a similar way with the following assumptions:

- Spore and crystal protein synthesis is catalyzed by the same polymerase (π^B or π^E, for weak and massive sporulation, respectively)
- Spore and crystal protein formation is controlled neither by ATP nor by GTP, since sufficient energy for polymerization is available at these times
- Breakdown of preexisting vegetative proteins supplies amino acids for formation of new proteins during sporulation
- The same signal controls the onset of sporulation as well as the turnover of vegetative protein
- Spore and crystal proteins are subject to moderate degradation processes.

Reaction rate expressions for sporulation phase processes are listed in Table 3.

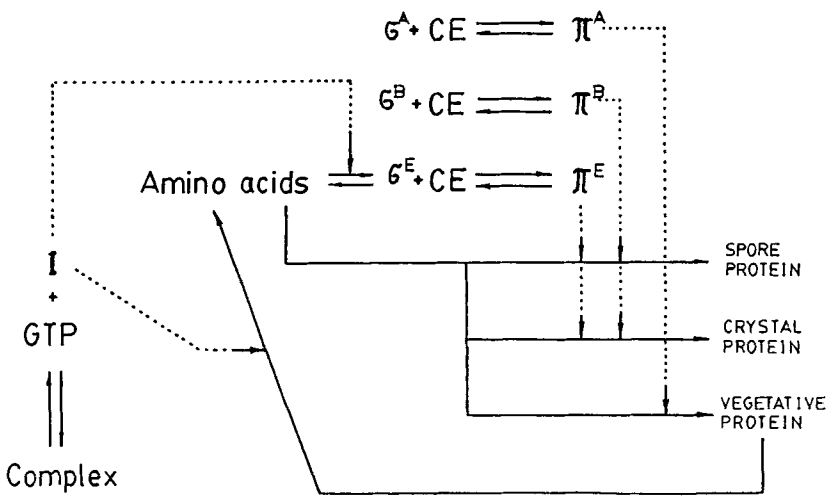

Fig. 3. Regulation of protein synthesis and sporulation.

Table 3
Kinetics of Sporulation Phase Processes

1. Spore and crystal protein formation - *weak sporulation*

$$r_{Sw} = k_{Sw}\,\pi^B\,\frac{AmA}{AmA + K_{AmA}}$$

$$r_{Cw} = k_{Cw}\,r_{Sw}$$

2. Vegetative protein turnover

$$r_T = k_T\,I\,P_V$$

3. Spore and crystal protein formation - *massive sporulation*

$$r_{Sm} = k_{Sm}\,\pi^E\,\frac{AmA}{AmA + K^*_{AmA}}$$

$$r_{Cm} = k_{Cm}\,r_{Sm}$$

4. Spore and crystal protein degradation

$$r_S^- = k_S^-\,P_S$$

$$r_C^- = k_C^-\,P_C$$

Governing Equations for Intracellular Components

Traditionally, the definition of the specific growth rate, μ, is based on the dry biomass concentration in broth (mass/vol). Hence, it is more convenient to use the mass fractions of dry biomass, a_i, for intracellular concentrations and express all intracellular reaction rates, r_j, in mass units per dry biomass per hour. Then, the balance equation for the i-th intracellular component takes the form:

$$\frac{da_i}{dt} = R_i - \mu a_i , \tag{4}$$

where the net formation rate of i-th component (R_i) is

$$R_i = \sum_j Y_{ji} r_j , \tag{5}$$

and the mass yield coefficients Y_{ji} can be evaluated from reaction stoichiometries. The second term on the right side of Eq. (4) accounts for dilution resulting from growth (*36*).

In structured models, the specific growth rate, μ, is not an independent quantity (*36*); it is determined by all intracellular reaction rates, since the summation of all mass balance equations (4) gives:

$$\mu = \sum_i R_i = \sum_i \sum_j Y_{ji} r_j = \sum_j \left(\sum_i Y_{ji} \right) r_j \tag{6}$$

SIMULATION OF BATCH FERMENTATIONS

Mass balance equations of extracellular components are usually written in terms of the concentrations c_i expressed in mass units per broth volume. For the batch operation, they have the following simple form:

$$\frac{dc_i}{dt} = R_i X \tag{7}$$

where the net reaction rates, R_i, are defined by Eq. (5) and X is the biomass concentration. In this particular case, the balance of biomass results directly from the definition of μ:

$$\frac{dX}{dt} = \mu X \tag{8}$$

In order to simulate batch fermentations, the system of differential equations (1), (4), (7) and (8) needs to be solved. Nonzero initial conditions were assumed for biomass, nutrients, and all intracellular vegetative

pools. The last-mentioned were taken as the concentrations typical for exponential growth. Zero initial conditions were assumed for extracellular products and both the sporulation proteins.

The original system of differential equations turned out to be numerically stiff, mostly because of a very high ATP, GTP, and $NADH_2$ turnover. To avoid the stiffness problems, we took advantage of the quasi-steady-state approximation (QSSA) in reference to the stiff variables. The justification for such a procedure is that the relaxation times for adaptation of ATP, GTP, and $NADH_2$ are much less than for the other pools (*37*). Additionally, to shorten the time of computation, the set of algebraic QSSA equations has been transformed into an equivalent set of differential equations.

RESULTS

Batch fermentations under conditions of glucose and ammonia limitation have been simulated. In both cases, kinetic parameters of vegetative growth were evaluated by applying balanced growth conditions, $da_i/dt = 0$, for all vegetative intracellular pools (*24*) and taking typical batch culture experimental values of $\mu = 0.8\ h^{-1}$ and $Y_{X/S} = 0.56$ g biomass/g glucose. The kinetic parameters of sporulation have been found while fitting available data (*38,39*) on the spore and crystal protein content at late sporulation (7–9 h after initiation). The estimated values of all model parameters have been presented in Table 4.

Some results of numerical simulation of glucose- and ammonia-limited batch cultures are presented in Figs. 4 and 5. More results, especially concerning variation of nucleotides and other intermediates, can be found in refs. (*24,32*).

Results of numerical simulation for the case of glucose-limited batch culture are presented in Fig. 4. For these simulations, the initial concentrations of glucose and ammonia were 4 g/dm^3 and 1 g/dm^3, respectively. The results were in qualitative agreement with the experimental observations reported in literature (*18,38,39*). After the exhaustion of glucose, utilization of ammonia ceased, and its level remained constant during sporulation. The final biomass concentration achieved was 2.6 g/dm^3. The amounts of vegetative protein in the cell exhibited a value of 48–49% during exponential phase, and it decreased almost linearly during the first part of sporulation. The total content of spore and crystal proteins from weak sporulation did not exceed 2%. A significant increase in the spore and crystal protein production was predicted about 1.2 h after exhaustion of glucose. About 8 h after that, the concentrations of spore and crystal proteins reached about 14 and 17% of dry weight, respectively. The concentration of GTP was around 0.9–1.0 m*M*. It increased to 1.6 m*M* about 30 min before glucose exhaustion and then rapidly dropped to zero.

Table 4
Maximum Reaction Rate and Equilibrium Constants

Maximum rate constants - reactions of vegetative phase [h^{-1}]:

$k_1 = 0.295$	$k_2 = 0.008$	$k_3 = 0.018$
$k_4 = 2.717$	$k_5 = 0.312$	$k_6 = 0.550$
$k_7 = 0.229$	$k_8 = 0.071$	$k_9 = 1277$
$k_{10} = 0.051$	$k_{11} = 6.838$	$k_{12} = 35.66$
$k_{13} = 0.556$	$k_{14} = 0.381$	$k_{15} = 0.002$
$k_{16} = 295.5$	$k_{17} = 33.26$	$k_{18} = 1.400$
$k_{19} = 0.029$		

Maximum rate constants - reactions of sporulation phase:

$k_{Sw} = k_{Sm} = 6.400\ h^{-1}$

$k_{Cw} = k_{Cm} = 1.217$

$k_T = 53.25\ h^{-1}$

$k_S^- = k_C^- = k_E^- = 0.062\ h^{-1}$

$k_E^+ = 2.098\ h^{-1}$

Equilibrium constants:

$K_A = 952$

$K_B = \infty \quad (K_B >> K_A)$

$K_E = \infty \quad (K_E >> K_A)$

$K_B / K_E = 0 \quad (K_E >> K_B)$

$K_I = 6.08 \times 10^{10}$

Similar behavior was predicted for ATP. During vegetative growth, the maximum yield of biomass from ATP (Y_{ATP}^{max}) and the maintenance coefficient (m_e) were nearly the same as those from theoretical considerations (23). The adenylate energy charge (E.C.) (*40*) was about 0.9.

The results of simulations involving nitrogen limitation are presented in Fig. 5. Here, the initial concentrations were 10 g/dm^3 for glucose and 0.1 g/dm^3 for ammonia. The predicted results again were in qualitative agreement with those experimentally observed for nitrogen limitation

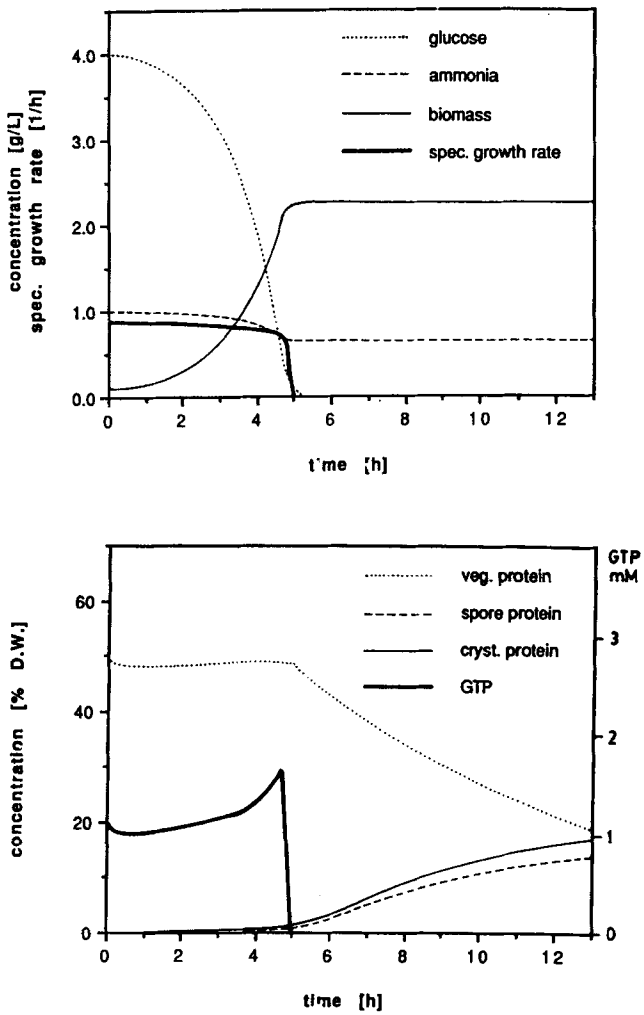

Fig. 4. Numerical simulation of batch fermentation—glucose limitation.

(*41*). After the exhaustion of ammonia, glucose concentration decreased almost linearly. The final biomass concentration was 0.6 g/dm^3. The lag between initiation and detection of massive sporulation was around 1.8 h. The amount of vegetative protein ranged from 48–52% during vegetative phase, which dropped to 23% after 9 h of sporulation. The final concentrations of spore and crystal proteins were 13 and 16%, respectively. The GTP pool decreased to about 8% of that before initiation and remained at a low level throughout sporogenesis. A GTP decrease of the same order was observed experimentally (*19,20*). The ATP concentration was nearly constant all the time (4.9 m*M*). Y_{ATP}^{max}, m_e, and E.C. revealed a behavior similar to that observed for glucose limitation.

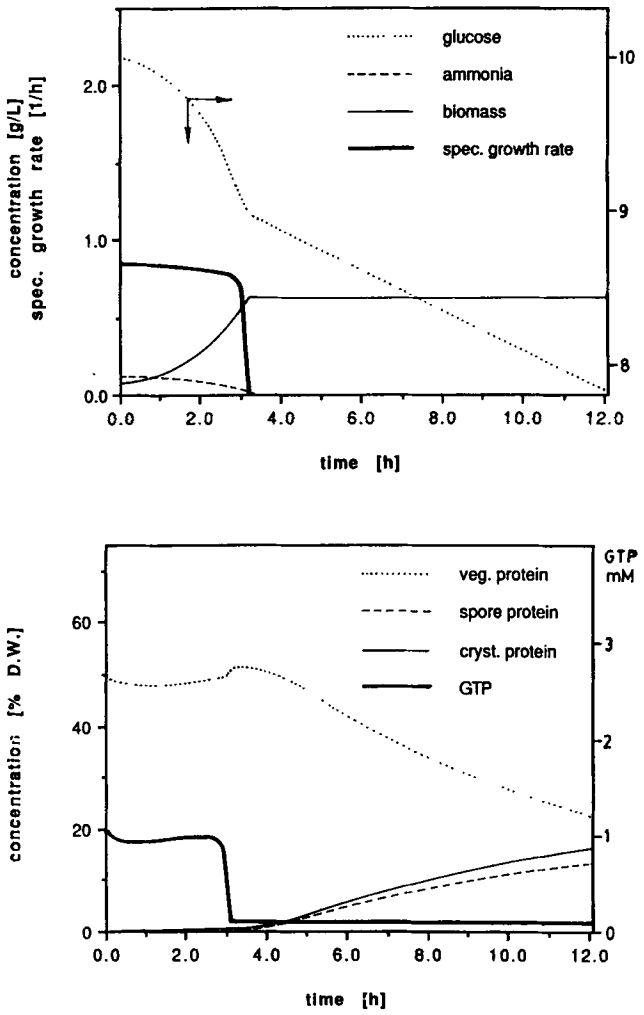

Fig. 5. Numerical simulation of batch fermentation—ammonia limitation.

CONCLUSIONS

A mathematical model of vegetative growth, sporulation, and crystal protein production in *Bt.* has been presented. This model incorporates the recorded essential features of metabolism as known for *Bacilli* and is an improvement over the previously developed model of Jeong et al. (3) for vegetative phase. The model predictions are in qualitative agreement with experimental observations. The major drawback of this model is the assumption of no energy requirement during sporulation, which stems from the lack of appropriate storage energy source modeled herein. One such compound commonly found for *Bacilli* is β-polyhydroxybutyrate (PHB) (42), which is produced from organic acids during vegetative phase

and is metabolized to carbon dioxide during sporulation. Incorporation of such a storage material will relax the need for the aforementioned assumption. It will also then eliminate another anomali of the present model, namely, the accumulation of organic acids during fermentation. In practice, they are produced (as also in this model), but are also consumed to produce PHB. This should be incorporated and is in progress.

REFERENCES

1. Shu, J. and Shuler, M. L. (1989), *Biotechnol. Bioeng.* **33,** 1117–1126.
2. Steinmeyer, D. E. and Shuler, M. L. (1989), *Chem. Eng. Sci.* **44,** 2017–2030.
3. Jeong, J. W., Snay, J., and Ataai, M. M. (1990), *Biotechnol. Bioeng.* **35,** 160–184.
4. Rowe, G. E. and Margaritis, A. (1987), *CRC Crit. Rev. Biotechnol.* **6,** 87–127.
5. Lüthy, P., Cordier, J.-L., and Fischer, H. M. (1982), *Microbial and Viral Pesticides* (Kurstak, E., ed.), Marcel Dekker, New York, pp. 35–74.
6. Andrews, R E., Jr., Faust, R. M., Wabiko, H., Raymond, K. C., and Bulla, L. A., Jr. (1987), *CRC Crit. Rev. Biotechnol.* **6,** 163–232.
7. Nickerson, K. W., Julian, G. S., and Bulla, L. A. (1974), *Appl. Microbiol.* **28,** 129–132.
8. Benoit, T. G. (1987), Ph.D. Thesis, Texas Tech. Univ., Lubbock.
9. Aronson, J. N., Borris, D. P., Doerner, J. F., and Akers, E. W. (1975), *Appl. Microbiol.* **30,** 489–492.
10. Megraw, R. E. and Beers, R. J. (1964), *J. Bacteriol.* **87,** 1087–1093.
11. Brown, T. D. K., Jones-Mortimer, M. C., and Kornberg, H. L. (1977), *J. Gen. Microbiol.* **102,** 327–336.
12. Liu, J.-K. and Jurtshuk, P., Jr. (1986), *J. Syst. Bacteriol.* **36,** 38–46.
13. Bulla, L. A., Jr., Bechtel, D. B., Kramer, K. J., Shethna, Y. I., Aronson, A. I., and Fitz-James, P. C. (1980), *CRC Crit. Rev. Microbiol.* **8,** 147–204.
14. Aubert, J. P., Millet, J., and Castoriadis-May, C. (1961), *C. R. Hebd. Seanc. Acad. Sci. (Paris)* **253,** 1731–1733.
15. Schaeffer, P., Millet, J., and Aubert, J. P. (1965), *Proc. Natl. Acad. Sci. USA* **54,** 704–711.
16. Dawes, I. W. and Thornley, J. H. M. (1970), *J. Gen. Microbiol.* **62,** 49–66.
17. Ollis, D. F. (1983), *Ann. N. Y. Acad. Sci.* **413,** 144–156.
18. Schulz, V., Schorcht, R., Ignatenko, Y. N., Sakharova, Z. V., and Khovrychev, M. P. (1985), *Stud. Biophys.* **107,** 43–51.
19. Federn, H. and Ristow, H. (1987), *Eur. J. Biochem.* **165,** 223–227.
20. Freese, E., Freese, E. B., Allen, E. R., Olempska-Beer, Z., Orrego, C., Varma, A., and Wabiko, H. (1985), *Molecular Biology of Microbial Differentiation* (Hoch, J. A. and Setlow, P., eds.), Am. Soc. Microbiol., Washington, DC, pp. 194–202.
21. Ingraham, J. L., Maalφe, O., and Neidhardt, F. C. (1983), *Growth of the Bacterial Cell,* Sinauer Associates, Inc. Publ., Sunderland, Mass.
22. Roels, J. A. (1983), *Energetics and Kinetics in Biotechnology,* Elsevier Biomedical Press, Amsterdam.
23. Stouthamer, A. H. (1973), *Antonie van Leewenhoek,* **39,** 545–565.
24. Starzak, M. and Bajpai, R. K. *Sporulating organisms. I. Modelling of vegetative growth,* in preparation.

25. Maalφe, O. and Kjeldgaard, N. O. (1966), *Control of Macromolecular Synthesis. A Study of DNA, RNA and Protein Synthesis in Bacteria,* Benjamin, New York.
26. Pine, M. J. (1970), *J. Bacteriol.* **103,** 207–215.
27. Shuler, M. L., Leung, S., and Dick, C. C. (1979), *Ann. N.Y. Acad. Sci.* **326,** 35–55.
28. Losick, R., Youngman, P., and Piggot, P. J. (1986), *Ann. Rev. Genet.* **20,** 625–669.
29. Errington, J. (1988), *Nature* **333,** 399–400.
30. Helmann, J. D. and Chamberlin, M. J. (1988), *Ann. Rev. Biochem.* **57,** 839–872.
31. Doi, R. H. (1982), *The Molecular Biology of the Bacilli* (Dubnau, D., ed.), pp. 71–109, Academic Press, New York.
32. Starzak, M. and Bajpai, R. K. *Sporulating organisms. II. Modelling of spore formation and related processes,* in preparation.
33. Vitkovic, L., Dhariwal, K. R., Freese, E., and Goldman, D. (1985), *FEMS Symp.* **18,** 177–195.
34. Mitchell, C. and Vary, J. C. (1989), *J. Bacteriol.* **171,** 2915–2918.
35. Sonenshein, A. L. (1985), *Molecular Biology of Microbial Differentiation* (Hoch, J. A. and Setlow, P., eds.), Am. Soc. Microbiol., Washington, DC, pp. 185–193.
36. Fredrickson, A. G. (1976), *Biotechnol. Bioeng.* **18,** 1481–1486.
37. Harder, A. and Roels, J. A. (1982), *Adv. Biochem. Eng.* **21,** 55–107.
38. Monro, R. E. (1961), *Biochem. J.* **81,** 225–232.
39. Lee, H. H., Lee, J. J., and Suh, J. H. (1986), *Sanop Misaengmul Hakhoechi* **14,** 329–334.
40. Atkinson, D. E. (1977), *Cellular Energy Metabolism and Its Regulation,* Academic Press, New York.
41. Liu, W.-M. and Bajpai, R. K.: paper presented at the 20-th Ann. Biotechnol. Eng. Symp., Manhattan, Kansas, April 21, 1990.
42. Dawes, E. A. and Senior, P. J. (1973), *Adv. Microb. Physiol.* **10,** 135–266.